Macromolecules
ARTICLE

Macromolecules **2010**, *43*, 10143–10151 **10143**
DOI: 10.1021/ma1004919

A Critical Size Ratio for Viscosity Reduction in Poly(dimethylsiloxane)−Polysilicate Nanocomposites

Randall G. Schmidt,*,† Glenn V. Gordon,† Cécile A. Dreiss,‡ Terence Cosgrove,⊥ Val J. Krukonis,§ Kara Williams,§ and Paula M. Wetmore§

†*Dow Corning Corporation, Midland, Michigan 48686-0994, United States,* ‡*Pharmaceutical Science Division, King's College London, SE1 9NH London, U.K.,* ⊥*School of Chemistry, University of Bristol, Cantock's Close, Bristol, BS8 1TS, U.K., and* §*Phasex Corporation, Lawrence, Massachusetts 01843, United States*

Received March 3, 2010; Revised Manuscript Received October 7, 2010

ABSTRACT: The zero-shear-rate viscosity η_0 of polymer−nanocomposites (PNCs) derived from entangled poly(dimethylsiloxane)s and rigid polysilicate nanoparticles were investigated as a function of molecular size and concentration. Narrow molecular weight fractions of polymer and nanoparticle were obtained by supercritical fluid extraction. Molecular weight properties were analyzed by size exclusion chromatography and the nanoparticle radius of gyration R_g was characterized by small-angle neutron scattering. All seven polysilicate fractions were smaller ($0.75 \leq R_g$, nm ≤ 2.1) than the five polymers ($3.0 \leq R_g$, nm ≤ 12). Relative to the polymer η_0 the PNC η_0 exhibited either plasticization (viscosity reduction) or reinforcement (viscosity increase). Only reinforcement was observed in PNCs based on the polymer below M_c—the critical molecular weight for chain entanglement effects to start influencing η_0—which included an increase in the PNC η_0 by over 3 orders of magnitude using 0.30 volume fraction of the largest nanoparticle. For polymers above M_c, the crossover from plasticization to reinforcement behavior could be described by a critical molecular-size ratio based on the unperturbed R_g of the nanoparticle and of the polymer. Viscosity reductions of up to 52% were achieved, and were more significant at the higher of the two nanoparticle concentrations studied. The critical nanoparticle-to-polymer R_g ratio at 298 K was 0.18 ± 0.006 and 0.13 ± 0.003 for a nanoparticle volume fraction of 0.17 and 0.30, respectively. A generalized form for the concentration dependent crossover ratio is proposed to account for perturbations in the molecular size of the PNC components that can be the basis for future studies. The effects of particle size polydispersity and temperature are discussed.

Introduction

The modification of polymers with particulate fillers is a conventional route for producing composites with enhanced performance properties often with a desired reduction in cost structure of commercial products. In terms of the influence of the particles on viscous and elastic properties, the primary variables have been expressed in the terms of its volume fraction ϕ_2 and maximum packing efficiency. Interaction (slip) at the particle−polymer interface and the Poisson's ratios will also impact the composite viscosity and modulus, respectively. The first description for the effect of a dilute concentration of (rigid, spherical) particles on the viscosity of a suspending medium was given by Einstein,[1,2] and extended in terms of a modulus by Smallwood.[3] Beyond the dilute regime, these limiting formulas have been corrected as particle−particle interactions become significant by using higher-order terms in ϕ_2 and a maximum-packing volume fraction ϕ_m.[4,5] The monotonic increase in viscosity or modulus with increasing ϕ_2 of rigid particles can be adequately described.[4] In addition, experimental results[3,6,7] confirmed the predictions to be independent of particle size although particle shape and size distribution will impact ϕ_m.[8−10]

In contrast, a reduction in the composite viscosity η_0 (relative to the polymer matrix viscosity $\eta_{0,1}$) has also been experimentally observed. Beginning in 1974, Malinskii et al.[11−14] reported $\eta_0/\eta_{0,1}$ values as low as 0.53 (47% reduction) upon addition of small amounts of filler ($\phi_2 \leq 0.02$) in polystyrene (PS), polypropylene, and plasticized poly(vinyl chloride), and that this "anomaly" was influenced by the type, size and symmetry of the filler as well as the nature of filler−polymer interactions. The proposed mechanisms for the phenomenon included the adsorption of polymer chains and the formation of additional free volume at the polymer−filler interface.

More recently, viscosity reductions were observed when nanometer-sized particles were incorporated into a polymeric matrix and referred to as a polymer−nanocomposite (PNC).[15−24] The apparent lack of universal trends in extending the rheological reinforcement of composites based on micrometer-sized colloidal fillers to nanosized fillers was often attributed to larger surface areas available for polymer−filler interactions when the particles are well dispersed and less than 100 nm in diameter.[25] Hence, it is not difficult to envisage the significance of the length and size scales of the composite components on rheology. Ganesan et al.[26] pointed to at least three—particle size (in terms of the hydrodynamic radius R), polymer radius of gyration $R_{g,1}$ and a polymer correlation length—while trying to determine the mechanisms responsible for the crossover from a regime of viscosity increase due to particle suspension to where the particles behave as a 'solvent' for the polymer. In comparing molecular dynamics (MD) simulations with experimental data, Kairn et al.[27] proposed the existence of a critical ratio of R-to-$R_{g,1}$ such that the composite zero-shear-rate viscosity $\eta_0(\phi)$ becomes approximately independent of ϕ_2.

One size scale of note detected experimentally was M_c, the polymer critical molecular weight for chain entanglement effects to start influencing η_0. An increase in the segmental mobility of polymer chains and a reduction in both η_0 and plateau

*Corresponding author. E-mail: r.g.schmidt@dowcorning.com.

Published on Web 11/02/2010

modulus G_N^0—consistent with the reptation model[28,29] used to describe entangled polymer dynamics—were reported when trimethylsilyl-treated polysilicate nanoparticles were dispersed over a certain concentration regime in siloxane polymers with weight-average molecular weights $\overline{M}_w$ well above its M_c.[15−19,30] It was hypothesized that these phenomena were due in part to the molecularly dispersed nanoparticles reducing the effective pairwise contacts of the polymer and effectively increasing the length between topological entanglements. Adsorption will lower $R_{g,1}$ if one chain is wound around one particle and hence will also reduce entanglements. However, this disentanglement mechanism does not appear to be universal since viscosity reduction exhibited by different PNCs[20,21,24] was unaccompanied by a decrease in G_N^0.

Additional length- and size-scale requirements to achieve viscosity reduction in PNCs were outlined by Tuteja et al.[22,31] including the need for $R_{g,1}$ to be greater than both the interparticle half-gap h and R to promote a stable dispersion (and avoid phase separation or agglomeration). Depletion flocculation must be considered when the adsorption energy is less than its critical value ($\chi_s < \chi_{sc}$), but this would not reduce the PNC viscosity below that of the pure polymer.[32] These guidelines were based on experimental systems using entangled PS polymers in combination with a variety of organic and inorganic nanoparticles.[20−23,31] In one particular combination,[23] viscosity reduction was proposed to occur when nanoparticles contribute to a constraint-release mechanism[33] by diffusing faster than the entangled polymer chains can reptate, which would imply that the nanoparticles are nonadsorbing. Additional experimental evidence for the role of the nanoparticles on the constraint-release mechanism may be found in the accompaniment to this paper where the power-law exponent in the $\eta_0 \sim \overline{M}_w$ relationship decreased from 3.4 for the unfilled polymer to 2.8 at $\phi_2 = 0.30$.[19] Qualitative agreement of enhanced nanoparticle diffusion (in an unentangled polymer) was provided by Liu et al.[34] using MD simulations to demonstrate that when $R < R_{g,1}$ diffusion is inversely proportional to R^3 instead of R because the local viscosity is less than the bulk viscosity and becomes independent of polymer molecular weight M but dependent on particle mass.

Kopesky et al.[24] ascribed a viscosity reduction at low nanoparticle loadings ($\phi_2 < 0.10$) to an increase in free volume from nonreactive polyhedral oligomeric silsesquioxanes (POSS) well dispersed in an entangled poly(methyl methacraylate) (PMMA). This was consistent with the proposed mechanisms of free volume being created at the nanoparticle−polymer interface[11,12,15−18] or via perturbation of the packing structure.[23,27]

MD simulations and theoretical treatments[26,27,35−38] also attempted to rationalize the mechanisms for viscosity reduction in PNCs—mostly using short, unentangled polymers—where, aside from ϕ_2, the nature of nanoparticle−polymer interactions, interparticle distance $2h$, and the ratio $R/R_{g,1}$ were investigated. Smith et al.[35] found viscoelastic properties to be described by a ϕ_2 dependence independent of particle size—consistent with conventional filled systems—and additional variables that accounted for the nature of the nanoparticle−polymer interaction and the specific interfacial area between the nanoparticle and the polymer matrix. The degree of confinement of the polymer matrix—defined by $R_{g,1}/2h$—did not appear to have a significant influence. Systems with nanoparticle−polymer interactions that were repulsive (relative to polymer−polymer interactions) exhibited a decrease in the dynamic shear modulus and viscosity consistent with a reduction in the polymer matrix density (i.e., free volume), and the resulting polymer dynamics were equally perturbed by the nanoparticles on all length scales.

Pryamitsyn and Ganesan[36] reported a strong dependence of (unentangled) polymer chain length to a nanoparticle-induced increase in relative viscosity, which was proposed to be from a mechanism of hydrodynamic slip of nonadsorbing polymer chains at the surface of the particle.[37] A continuum model that took into account slip was proposed by Ganesan et al.[26] wherein the polymer length scale controlling the transition from plasticization to reinforcement was $R_{g,1}$ and the reptation tube diameter d_t[25,26] for unentangled and entangled melts, respectively. For the former, viscosity reduction for neutral or weakly interacting nanoparticles was predicted to scale with polymer volume fraction ϕ_1 if $R/R_{g,1} \ll 1$, sometimes referred to as the protein limit, in accordance with the dilution model. For the latter, the decrease in viscosity would be accentuated from the loss of entanglements such that it scaled with $\phi_1^{11/3}$ for $R/d_t \ll 1$.

Sen et al.[38] interpreted simulated viscosity-reduction results at low ϕ_2 due to repulsive polymer−particle interactions. This was based on MD simulations[39] that revealed enhanced diffusivity of polymer chains within $R_{g,1}$ distance from the nanoparticle surface, and is consistent with data from our experimental siloxane PNC systems.[19]

The merits brought about by this viscosity−reduction phenomenon include improved processability while affording the flexibility to optimize performance properties by varying the concentration of the nanoparticles in a regime where there is no substantial aggregation. The potential of PNCs to enhance traditional performance attributes or manifest new ones—such as the ability to self-heal in response to mechanical damage—are highlighted and referenced in several publications cited herein. Improvements were reported for PS−fullerene systems in terms of viscoelastic damping, thermal stability, and electrical conductivity.[23] PNCs based on POSS covalently tethered on a polymeric backbone have generated significant attention with respect to molecular reinforcement and its effect on physical properties.[24,40] Polysilicate nanosized particles have long been used to tune the viscoelasticity and enhance the durability of linear siloxanes in various commercial applications including pressure-sensitive adhesives and release linears.[41,42]

In the companion paper, the study of the influence of polymer molecular weight on the dynamics of PNCs based on poly(dimethylsiloxane) PDMS and polysilicate fillers was reported.[19] This paper extends that study to the molecular size of both PNC components. A trimethysilyl-treated polysilicate was fractionated by molecular size and characterized by small-angle neutron scattering. Entangled PDMS of varying M was used as the matrix. In this study, the PNC $\eta_0(\phi)$ was characterized to add insight on the critical size scales and parameters that enable PNC viscosity reduction. It is recognized that many parameters including the type and extent of particle/polymer interactions, the particle shape and size distribution, and polymer backbone flexibility will impact the viscosity of a given PNC. Hence, identifying critical size scales for viscosity reduction that apply universally to PNCs is unlikely. However, the compatibility over broad compositional ranges, the absence of specific particle/polymer interactions and the high degree of flexibility of the PDMS backbone make the poly(dimethylsiloxane) (PDMS)/ polysilicate system attractive for investigating factors that control PNC viscosity.

Experimental Section

Materials. A trimethylsilylated polysilicate, obtained from the acid-catalyzed polymerization of sodium silicate in a process described previously,[43] was fractionated from its bulk form into narrow molecular weight fractions using supercritical fluid (SCF) extraction (Phasex Corporation, Lawrence, MA). The general equipment and methodology for carrying out SCF extraction using carbon dioxide were explained in detail elsewhere.[44] Using a charge of 1.071 kg of the bulk polysilicate, 10 fractions were extracted with a total yield of 98.9%. Figure 1 compares the molecular weight profiles obtained by size exclusion chromatography (SEC) for the bulk polysilicate and seven fractions (labeled according to the fractionation sequence)

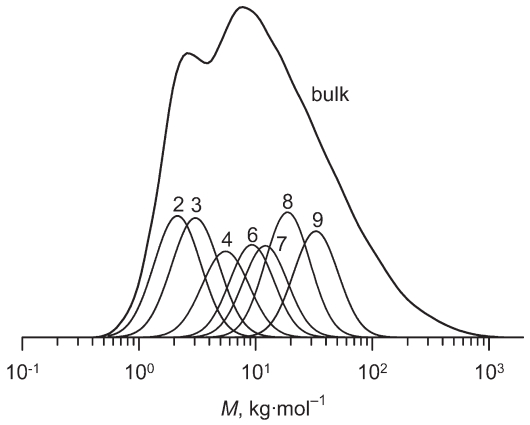

Figure 1. Molecular weight profiles of the polysilicate fractions used in this study obtained via SCF extraction from a bulk polysilicate.

Table 1. Physical Properties of Polysilicate Materials

Material Designation	$\overline{M}_{w,2}$ (kg·mol^{-1})	$\overline{M}_w/\overline{M}_n$	$R_{g,2}$[a] (nm)	ρ_2(293 K) (kg·m^{-3})
S2	2.4	1.2	0.75	1113
S3	3.7	1.2	0.87	1160
S4	5.8	1.2	1.0	1186
S6	9.6	1.1	1.3	1208
S7	12.5	1.1	1.5	1216
S8	17.9	1.1	1.7	1225
S9	30.2	1.1	2.1	1232
bulk	19.0	4.0	1.9	N/A

[a] Calculated from the Guinier analysis of SANS experimental data.

chosen for this study. The chosen fractions were amorphous powders at room temperature, and the physical properties—characterized by analytical methods described in the following sections—are summarized in Table 1.

Five trimethylsiloxy-end blocked PDMS polymers, with physical properties listed in Table 2, were used to make PNCs with the polysilicate fractions. Four narrow polymer fractions were derived from a Dow Corning 12 500 cSt 200 Fluid (lot 1812258) using SCF extraction whereas a fifth polydisperse polymer was obtained from in-house stock. The experimental details were documented elsewhere.[19]

For each PNC series, the components were dissolved in reagent-grade xylenes to assist with dispersion of the polysilicate powders at target volumetric ratios and mixed overnight on a tumbling device. To remove the solvent, the blends were exposed as thin films in a forced-air oven at 393 K for 16 h followed by 16 h under full vacuum at 343 K. The resulting solvent-free PNCs were clear, colorless and shelf stable. Measurements were conducted at least one month after PNC preparation. Following the convention for composites,[4] the subscripts 1 and 2 denote the polymer and nanoparticle components, respectively.

Characterization. *Size Exclusion Chromatography*. The polysilicate molecular weight properties—including the number-average value $\overline{M}_n$—were determined by a size exclusion chromatography (SEC) set up that included a Waters 2695 Separation Module equipped with two (300 mm ×75 mm) Polymer Laboratories Mixed-D columns (linear separation range of 0.2 to 400 kg·mol^{-1}) calibrated with SCF-derived polysilicate molecular weight fractions, a Miran1A-CVF HPLC infrared detector (9.1 μm; 1099 cm^{-1} Si−O−Si), and HPLC-grade chloroform as the eluant at 308 K.

The molecular weight properties of PDMS polymers were analyzed by SEC instrumentation that consisted of a Waters 515 pump, 717 autosampler, and 2410 differential refractometer. The separation was made using two (300 mm ×7.5 mm) Polymer Laboratories PLgel 5-μm Mixed-C columns (separation range of 0.20 to 2000 kg·mol^{-1}) preceded by a PLgel 5-μm guard column

Table 2. Physical Properties of PDMS Materials

material designation	$\overline{M}_{w,1}$ (kg·mol^{-1})	$\overline{M}_w/\overline{M}_n$	$R_{g,1}$[a] (nm)	ρ_1(293 K) (g·cm^{-3})	$\eta_{0,1}$(298 K) (Pa·s)
13K	13.0	1.1	3.0	0.971	0.142
47K	46.8	1.4	5.7	0.975	2.45
67K	66.7	1.3	6.9	0.975	7.36
109K	109.	1.2	8.8	0.976	42.9
216K*p*	216.	2.1	12.3	0.978[b]	977.

[a] Calculated from the relationship 0.839 $\overline{M}_w^{0.5}$ at 298 K.[45] [b] On the basis of historical data for commercial-grade PDMS.

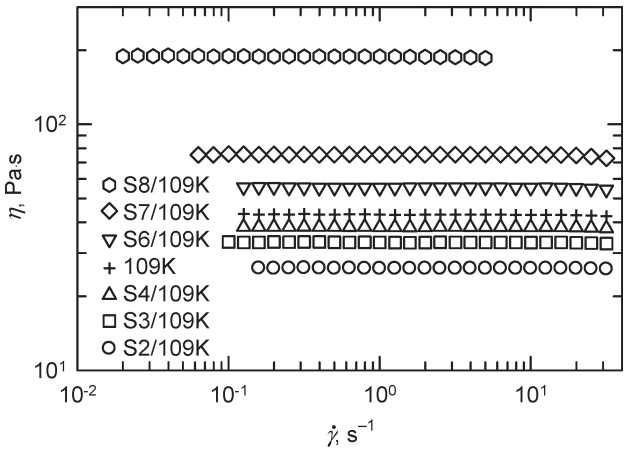

Figure 2. Rate dependence of the steady shear viscosity of a 109K PDMS (+) and PNCs prepared from it using a 0.30 volume fraction of polysilicate nanoparticles.

(50 mm ×7.5 mm). HPLC-grade toluene flowing at 1.0 mL·min^{-1} was the eluant with the columns and detector at 318 K. Solutions in toluene were prepared at 0.5% w/v polymer and filtered through a 0.45-μm PTFE syringe filter into glass autosampler vials. A 50-μL injection volume was used and data were collected for 25 min and processed using PE Nelson Access* SEC software. Molecular weight averages were determined relative to a third-order polynomial calibration curve derived from PS calibration standards covering a molecular weight range of 0.58−1290 kg·mol^{-1}.

Density. Material density was measured at 293 K using an Anton PAAR DMA48 density meter with a specified accuracy and precision of 1×10^{-1} and 3×10^{-2} kg·m^{-3}, respectively. For the polysilicates, a concentration series of solutions in tetrahydrofuran was prepared up to 17 wt % solute in order to extrapolate density following a procedure reported elsewhere.[46]

Small-Angle Neutron Scattering. SANS experiments were conducted at the Berlin Neutron Scattering Center (Hahn-Meitner-Institut, Germany) using the V4 instrument installed at the curved neutron guide NL3 A (Ni coated, cutoff wavelength $\lambda = 0.38$ nm) with incoming neutrons monochromatized by a mechanical velocity selector, a two-dimensional position sensitive ^{3}He gas detector of 0.64×0.64 m^2, sample−detector distances positioned at 4 and 1 m, and a neutron wavelength of 0.605 nm to cover a scattering vector Q range from 0.03 to 3.7 nm^{-1}.

The size and shape of the nanoparticles were characterized by dispersing the polysilicate fractions in deuterated toluene ($\phi_2 = 0.02$) to achieve maximum contrast. This concentration was considered high enough to achieve sufficient signal from the nanoparticles but low enough to avoid the influence of interparticle interactions. The neutron-scattering length density of the nanoparticles ρ_p was fixed to 1.06×10^{-4} nm^{-2} and the difference relative to toluene-d ($\rho_m = 5.67 \times 10^{-4}$ nm^{-2}) was not anticipated to significantly impact the result of the fits as the contrast was simply a scaling factor for the intensity.

Rheology. Steady-shear viscosity was characterized as a function of shear rate to determine η_0 at 298 K using TA Instruments RDA-type rheometers equipped with spring transducers that

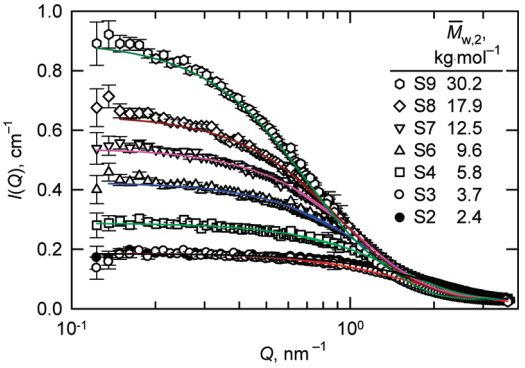

Figure 3. Neutron scattering intensity of polysilicate nanoparticles in *d*-toluene. Lines represent fits to spherical ($\overline{M}_{w,2} < 5.8$ kg·mol^{-1}) and cylindrical ($\overline{M}_{w,2} \geq 5.8$ kg·mol^{-1}) models.

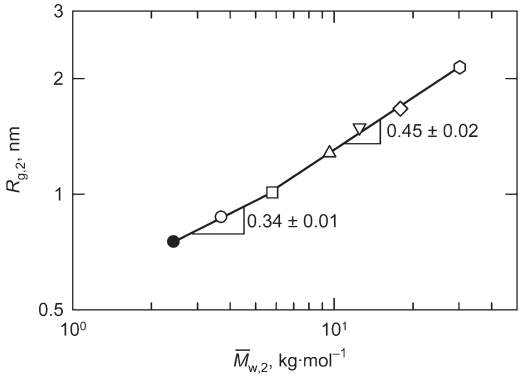

Figure 4. Molecular weight dependence of the radius of gyration of polysilicate fractions.

provided a torque range of 0.02−200 mN·m, a forced-convection oven, and 25- or 50 mm-diameter cone-and-plate fixtures with nominal cone angles of 0.10 and 0.04 radians, respectively. The Newtonian region of all the polymers and PNCs was within the accessible shear-rate range of the rheometers as shown in Figure 2, for example, for a PNC series using $\phi_2 = 0.30$ in a 109K PDMS. The data reported here were all based on η_0. Newtonian behavior was observed for all of the PNCs over the entire shear rate range consistent with a system that is devoid of significant particle agglomeration.

Results and Discussion

SANS Characterization of Size and Shape of Polysilicate Nanoparticles. Figure 3 shows the SANS scattering results from seven fractions—with fractions S2 (●) and S3 (○) displaying significant overlap. The overall size of each polysilicate fraction was obtained from the Guinier analysis[47] of the scattering intensity I as a function of the scattering vector Q in the region $QR_g < 1$.

$$\ln I(Q) \sim -\frac{Q^2 R_g^2}{3} \quad (1)$$

The calculated R_g values for the polysilicates are provided in Table 1. Figure 4 plots $R_{g,2}$ as a function of $\overline{M}_{w,2}$ on logarithmic scales: for $\overline{M}_{w,2} < 5.8$ kg·mol^{-1},

$$R_{g,2} = 0.55(\pm 0.004)\overline{M}_{w,2}^{\,0.34 \pm 0.01} \quad (2)$$

which suggested that the polysilicate would be predominantly spherical; at higher $\overline{M}_{w,2}$, there was a shift in the scaling exponent

$$R_{g,2} = 0.46(\pm 0.02)\overline{M}_{w,2}^{\,0.45 \pm 0.02} \quad (3)$$

indicative of more asymmetrically shaped particles.

The scattering data from the two lowest M fractions could be fitted to a spherical-shape model

$$I(Q) = 9(\rho_p - \rho_m)^2 \phi V_p \left[\frac{\sin QR_g - QR_g \cos QR_g}{(QR_g)^3}\right]^2 \quad (4)$$

where ϕ is the volume fraction of the dispersion, and V_p the particle volume. The results are shown in Figure 3 as solid lines with a log-normal size distribution of sizes such that the calculated polydispersity was ca. 10%, and a $R_{g,2}$ of 1.0 and 1.2 nm was calculated for the S2 and S3 fractions, respectively. The Guinier approximation ignores the influence of size distribution and does not make assumptions on the particle shape. Therefore, if the particles are elongated the R_g will be considerably larger than if it were spherical given the definition $R_g^2 = \Sigma m_i r_i^2 / \Sigma m_i$, and the dependence on distance of the mass of segments (m) from the center of mass (r) squared. It could be envisaged that these spherical nanoparticles are made up of a silicate ($SiO_{4/2}$) polyhedral core surrounded by a shell of trimethylsiloxy groups.

For the higher M fractions, significantly higher polydispersity values were required in the attempt to better describe the scattering results and, in particular, to fit the low-Q region (not shown). However, it was evident that the higher M fractions displayed an asymmetry in shape that could not be taken into account by a model based on a simple sphere. Therefore, a cylinder model[48] was applied next with radius R and length l as the main fitting parameters. This model does not accommodate for a polydispersity of particle sizes, but better fits to the scattering data—as measured by the merit value χ^2—were obtained by allowing for slight adjustments in ϕ. The results for $\overline{M}_{w,2} \geq 5.8$ kg·mol^{-1} are depicted in Figure 3 as solid lines whereas the fitted parameters are summarized in Table 3. Also included in Table 3 are calculated values for an aspect ratio $l/2R$ to describe the asymmetry of the nanoparticles, which can be attributed to interconnected trains of lower-M spherical particles, and R_g calculations for a cylinder (last column) for comparison with R_g obtained by the Guinier approximation (Table 1).

Therefore, the higher M fractions of polysilicate nanoparticles can be better described as cylinders. It is quite probable these were more polydisperse in size and shape as evidenced from the decreasing quality of the fits (χ^2), and the necessity of using lower values for ϕ relative to 0.02. This could also suggest the occurrence of slight aggregation. The suitability of the cylinder model was also demonstrated by a good linear correlation between the cylinder volume multiplied by the measured density $\pi R^2 l \cdot \rho$ and $\overline{M}_{w,2}$ ($r^2 = 0.999$).

The SANS results pointed to a structural evolution with increasing M such that the data could be rationalized by a bimodal molecular weight distribution of the bulk polysilicate in Figure 1: spherical nanoparticles in the first, lower M mode, and cylindrical nanoparticles made up of linked spheres in the second mode.

Polymer Nanocomposite Viscosity. The PNCs were prepared at 17 and 30 vol % particle loadings. In the companion paper,[19] several characteristics of this PNC system were brought forward as indirect evidence that particle aggregation is not appreciable. Table 4 summarizes the PNC η_0 at 298 K as a function of the $\overline{M}_w$ of each component and ϕ_2. Whereas five entangled polymers were used, only four satisfied the condition $\overline{M}_w > M_c$, where $M_c \sim 29$ kg·mol^{-1}

Table 3. Numerical Results for Fitting a Cylinder Model to SANS Data for Polysilicates

	Fitting Parameters for Cylinder Model					R_g for a cylinder
polysilicate	R (nm)	l (nm)	ϕ	χ^2	$l/2R$	$\sqrt{(R^2/2)+(l^2/12)}$(nm)
S4	0.97	3.08	0.014	1.7	1.59	1.12
S6	1.13	3.90	0.012	1.5	1.73	1.38
S7	1.20	4.44	0.012	6.0	1.85	1.54
S8	1.28	5.28	0.011	25.	2.06	1.77
S9	1.41	7.19	0.009	73.	2.55	2.30

Table 4. Polymer and Nanocomposite Viscosity as a Function of Molecular Weight and Volume Fraction

	η_0(298 K), Pa·s					
	$\phi_2 = 0.17$		$\phi_2 = 0.30$			
Polysilicate	67K	109K	13K	47K	109K	216Kp
none	7.36	42.9	0.142	2.45	42.9	977.
S2	6.19	31.7	0.316	2.52	26.0	471.
S3	6.73	34.1	0.403	3.30	33.1	527.
S4	7.05	35.6	0.643	4.35	38.2	543.
S6	7.83	38.6	1.94	8.25	55.4	677.
S7	8.17	40.3	4.02	16.8	75.3	827.
S8	8.92	43.3	14.6	58.1	190.	1120.
S9	11.4	47.2	321.	1720.	2760.	3060.

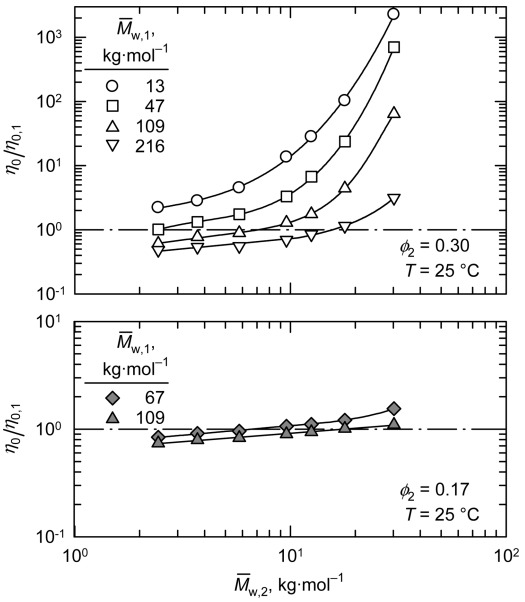

Figure 5. Relative viscosity of PDMS nanocomposites at 298 K as a function of polysilicate $\overline{M}_w$ for nanoparticle volume fractions of 0.30 (top) and 0.17 (bottom).

for PDMS.[49] Fetters et al.[45] cited SANS-measured and calculated values of the molecular weight for the onset of polymer entanglements, M_e, for PDMS at 298 K as 9.6 kg·mol^{-1} and 12.0 kg·mol^{-1}, respectively.

Effect of Polysilicate Molecular Weight $\overline{M}_{w,2}$. Figure 5 uses a logarithmic scale to plot the impact of $\overline{M}_{w,2}$ on the relative PNC viscosity, $\eta_0/\eta_{0,1}$, for $\phi_2 = 0.30$ in four polymers spanning a $\overline{M}_{w,1}$ range from 13 to 216 kg·mol^{-1} (top), and for $\phi_2 = 0.17$ in two polymers (bottom). For each polymer, $\eta_0/\eta_{0,1}$ increased monotonically with increasing $\overline{M}_{w,2}$. However, the effect of $\overline{M}_{w,2}$ on enhancing $\eta_0/\eta_{0,1}$ diminished with increasing $\overline{M}_{w,1}$. For each $\overline{M}_{w,2}$, the impact of a constant ϕ_2 on $\eta_0/\eta_{0,1}$ varied with increasing $\overline{M}_{w,1}$: some PNCs exhibited the typical reinforcement of the base polymer, or $\eta_0/\eta_{0,1} > 1$; however, the plasticization condition $\eta_0/\eta_{0,1} < 1$ was evident in other systems.

For the 13K PDMS with $M_e < \overline{M}_{w,1} < M_c$, $\eta_0/\eta_{0,1} > 1$ was found for all polysilicate fractions at $\phi_2 = 0.30$ and increased over 3 orders of magnitude using the highest M nanoparticle (S9). This trend was consistent with findings from previous studies using polydisperse bulk form of polysilicates.[15,18,51] For the four polymers with $\overline{M}_{w,1} > M_c$, $\eta_0/\eta_{0,1} \leq 1$ was observed over a certain $\overline{M}_{w,2}$ range where an eventual crossover to reinforcement behavior shifted to higher $\overline{M}_{w,2}$ with increasing $\overline{M}_{w,1}$. The data from PNCs based on the 109K PDMS also revealed a shift in the crossover to a lower $\overline{M}_{w,2}$ with the higher nanoparticle concentration ($\phi_2 = 0.30$).

The greatest viscosity reduction (52%) was expectedly achieved using the combination of the smallest nanoparticle (S2) and the highest M PDMS (216Kp). For the 47K polymer, $\eta_0(\phi_2 = 0.30)/\eta_{0,1} \sim 1$ at the lowest $\overline{M}_{w,2}$ (S2) suggesting that viscosity reduction could occur at lower ϕ_2. Within the plasticization regime, a power-law relationship between $\eta_0/\eta_{0,1}$ and $\overline{M}_{w,2}$ could be used with a power-law exponent that appeared to depend on $\overline{M}_{w,1}$. For $\phi_2 = 0.30$, $\eta_0/\eta_{0,1}$ scaled as $\overline{M}_{w,2}^{0.44 \pm 0.07}$ ($\overline{M}_{w,2} < 7$ kg·mol^{-1}) and $\overline{M}_{w,2}^{0.32 \pm 0.06}$ ($\overline{M}_{w,2} < 16$ kg·mol^{-1}) for the 109K and 216Kp polymers, respectively. For $\phi_2 = 0.17$, $\eta_0/\eta_{0,1}$ scaled as $\overline{M}_{w,2}^{0.17 \pm 0.01}$ ($\overline{M}_{w,2} < 7$ kg·mol^{-1}) and $\overline{M}_{w,2}^{0.15 \pm 0.01}$ ($\overline{M}_{w,2} < 18$ kg·mol^{-1}) for the 67K and 109K polymers, respectively. The polysilicate $\overline{M}_w$ limit in parentheses marked the crossover into the plasticization regime of each polymer. For the PNCs derived from a 109K PDMS, the power-law exponents point to an enhanced viscosity reduction at the higher ϕ_2. Unlike the proposed condition of spherical nanoparticles,[21] the increasing asymmetry of the higher M polysilicates did not appear to significantly impact the viscosity reduction mechanism.

Effect of Molecular Size R_g. In the following section, the nanoparticle size will be expressed in terms of $R_{g,2}$ as determined from the Guinier analysis of the SANS data, and ranged from 0.75 to 2.1 nm (Table 1). For the PDMS component, $R_{g,1}$ values at 298 K listed in Table 2 were calculated from the SEC-derived $\overline{M}_w$ data using the relationship from SANS measurements[45]

$$R_g = 0.839\overline{M}_w^{0.5} \quad (5)$$

where R_g is expressed in nm and $\overline{M}_w$ in kg·mol^{-1}. Therefore, $R_{g,2}/R_{g,1}$ was less than unity for any polymer−polysilicate combination. In addition, $d_t > R_{g,2}$ given cited d_t values from 7.2 to 7.4 nm at 298 K.[45,51]

For another proposed[22,31] length-scale parameter for viscosity reduction, $R_{g,1} > h$, h can be estimated from the relationship with the boundary condition $\phi_2 \leq \phi_m$

$$h/R = (\phi_m/\phi_2)^{1/3} - 1 \quad (6)$$

where $R = \sqrt{5/3}R_g$ assuming a spherical particle and ϕ_m can range from 0.59 to 0.64 for loose through dense random packing.[4,5] This condition was satisfied given $R_{g,1} = 3$ nm for the smallest (13K) polymer and the nanoparticle concentrations

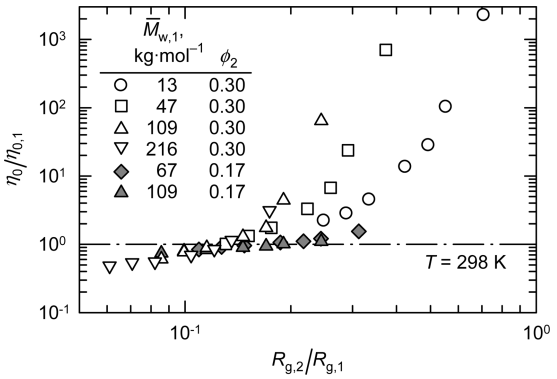

Figure 6. Relative viscosity of PDMS nanocomposites at 298 K as a function of the ratio of polysilicate R_g to PDMS R_g and nanoparticle volume fraction.

used in this study: $0.24 < h(\phi_2 = 0.30)$, nm < 0.79 and $0.50 < h(\phi_2 = 0.17)$, nm < 1.50.

Figure 6 replots the $\eta_0/\eta_{0,1}$ results in Figure 5 as a function of $R_{g,2}/R_{g,1}$, which ranged from 0.06 to 0.71. It was already noted that the largest viscosity reduction was obtained from the S2/216K*p* PNC, which corresponded to the lowest $R_{g,2}/R_{g,1}$ (0.06), while the greatest reinforcement in $\eta_0/\eta_{0,1}$ was produced from the S9/13K combination having the largest $R_{g,2}/R_{g,1}$ (0.71). The $R_{g,2}/R_{g,1}$ dependence of $\eta_0/\eta_{0,1}$ in the reinforcement regime was a strong function of $R_{g,1}(\overline{M}_{w,1})$ in contrast to the trend found in the plasticization regime.

At each ϕ_2, the collection of data from different PNCs converged at a critical $R_{g,2}/R_{g,1}$ ratio as the relative viscosity crossed over from the plasticization and into the reinforcement regime: $\eta_0/\eta_{0,1} = 1$. This transition occurred at $R_{g,2}/R_{g,1} = 0.13 \pm 0.003$ for $\phi_2 = 0.30$ where, in the plasticization regime, there was a strong size-ratio dependence on relative viscosity: $\eta_0/\eta_{0,1} \sim (R_{g,2}/R_{g,1})^{0.90\pm0.11}$. For $\phi_2 = 0.17$, $R_{g,2}/R_{g,1}$ crossed over at 0.18 ± 0.006, and the effect of $R_{g,2}/R_{g,1}$ on viscosity reduction was weaker: $\eta_0/\eta_{0,1} \sim (R_{g,2}/R_{g,1})^{0.37\pm0.04}$ in accordance with power-law relationships found with $\overline{M}_{w,2}$.

The crossover at $\eta_0/\eta_{0,1} = 1$ can also be viewed in terms of $h/R_{g,1}$, which can be estimated using eq 6 and assuming values for ϕ_m spanning the range for random packing. For $\phi_2 = 0.17$, $h/R_{g,1} = 0.12 \pm 0.01$. For $\phi_2 = 0.30$, however, the PNCs based on the polymer fractions 47K and 109K appeared to converge at $h/R_{g,1} = 0.045 \pm 0.006$ whereas the crossover occurred at $h/R_{g,1} = 0.035 \pm 0.005$ for the 216K*p*-based PNCs.

For the PNCs using the 13K PDMS (○), a crossover (in violation of the stipulation $\overline{M}_{w,1} > M_c$) would hypothetically occur at $R_{g,2} = 0.39$ nm, which from eq 2 would correspond to $\overline{M}_{w,2} = 0.35$ kg·mol^{-1}. This extrapolated $\overline{M}_{w,2}$ is below the lower limit for this type of material and anywhere in this M vicinity the silicate would be oligomeric and liquid at 298 K.[15,50]

The viscosity-reduction results reported by Mackay et al.[21−23] for PNC systems at 170 °C using a PS ($\overline{M}_w > M_c$, $R_{g,1} = 17$ nm) revealed the following: (1) $0.18 \le \eta_0/\eta_{0,1} \le 0.64$ for three different cross-linked PS nanoparticles ($0.13 \le R_{g,2}/R_{g,1} \le 0.23$) in the concentration range $0.05 \le \phi_2 \le 0.20$;[21] (2) $\eta_0\,(\phi_2 \sim 0.06)/\eta_{0,1} \sim 0.2$ using C_{60} fullerene ($R/R_{g,1} \sim 0.02$);[22] (3) $\eta_0\,(\phi_2 \sim 0.01)/\eta_{0,1} \sim 0.1$ for Fe_3O_4 magnetite ($0.29 < R/R_{g,1} < 0.58$);[22] and, (4) $\eta_0\,(\phi_2 \sim 0.08)/\eta_{0,1} \sim 0.4$ with oleic acid stabilized cadmium selenide quantum dots ($R/R_{g,1} \sim 0.27$).[23] For the POSS−PMMA PNCs investigated by Kopesky et al.,[24] the size ratio was approximately 0.20 and $\eta_0\,(\phi_2)/\eta_{0,1} < 1$ at 190 °C when using a cyclohexyl-POSS at $\phi_2 < 0.06$ or an isobutyl-POSS at $\phi_2 < 0.10$. Hence, these experimental trends were consistent with the results depicted in Figure 6 illustrating that while ϕ_2 should be taken into account, $\eta_0/\eta_{0,1}$ decreased with decreasing $R_{g,2}/R_{g,1}$.

MD simulations of PNCs yielded decreases in viscosity below that of the polymer only when the nature of the nanoparticle−polymer interactions was repulsive. Smith et al.[35] used a model consisting of a matrix of coarse-grained bead-necklace unentangled chains containing a single, roughly spherical nanoparticle such that $0.63 \le \eta_0/\eta_{0,1} \le 0.89$ as ϕ_2 increased from 0.15 to 0.24. In contrast to the experimental systems cited herein, these results were obtained with the following length-scale characteristics: $1.75 \le R/R_{g,1} \le 3.47$; and, $0.75 \le R_{g,1}/h \le 1.12$. On the basis of $R/R_{g,1} \sim 2.5/4.7$ ($R_{g,2}/R_{g,1} \sim 0.4$) with chain dynamics in the crossover regime between Rouse and reptation behavior, Sen et al.[38] found moderate increases in viscosity for $\phi_2 = 0.08$ and 0.15 consistent with the experimental response measured here using the 13K polymer. However, $\eta_0/\eta_{0,1} < 1$ was simulated when the nanoparticle concentration was reduced to $\phi_2 = 0.02$.

Aside from its macroscopic effect on viscosity, it should be realized that the concentration dependence on the crossover size ratio reported here was based on unperturbed molecular dimensions. Cosgrove et al.[52] used SANS and MD simulations to emphasize the importance of relative size on the dynamics of polymer adsorption. The interactions between the polysilicate nanoparticle and PDMS polymers have been investigated by nuclear magnetic resonance (NMR) and scattering techniques.[15−18,50,53] NMR spin−spin relaxation results found the presence of perturbed chains with restricted segmental mobility that increased with ϕ_2. Below a certain nanoparticle concentration, the component attributed to trains increased with ϕ_2, but noting the possibility that a proportion of the loops and tails also with highly restricted mobility but invisible in the NMR relaxation time scale would also have been assigned as trains. SANS data suggested the formation of (nanoparticle) core− (polymer) shell structures and detected no evidence of other structures such as decorated chains. The core−shell structures all exhibited R_g values less than $2R_{g,1}$ of isolated polymer coils. Within the context of the reptation theory, a quasielastic neutron scattering experiment has a spatial range limiting observation to local motion within the tube thereby ignoring effects from the entanglement mesh; only a progressive slowing down of polymer motion due to adsorption on polysilicate nanoparticles was detected.

Surve et al.[54] used a polymer self-consistent field theory to demonstrate significant $R/R_{g,1}$ dependence of polymer adsorption—predominantly in the form of tails extended up to approximately $2R_{g,1}$—in the region $0.1 < R/R_{g,1} < 1$. Monte Carlo (MC)[55−60] and MD[38,61,62] modeling simulations likewise point toward an ordering of chains/trains into densely packed shells. Therefore, it may be reasonable to assume that particle size will effectively increase by $R_{g,2} + \delta$, where δ is a hydrodynamic corona of polymer chains that could depend on ϕ_2 within the limit defined by h, and scale with $\overline{M}_{w,1}$.[63] Roberts et al.[15,50] used a nanoparticle similar to the bulk polysilicate in this study ($R_{g,2} = 2.2$ nm) and estimated δ via pulsed-field gradient spin echo NMR to be approximately independent of ϕ_2 (≤ 0.35): 0.35 ± 0.04 nm and 0.47 ± 0.11 nm for 5.2 kg·mol^{-1} and 12.2 kg·mol^{-1} PDMS, respectively. In general, δ increases with increase in particle size until $R_{g,2} > R_{g,1}$.[64] δ should be independent of ϕ up to the point where there are significant particle−particle interactions then (assuming repulsion) should contract.[65]

The influence of nanoparticle fillers on polymer length and size scales is less understood. From the reptation theory, the

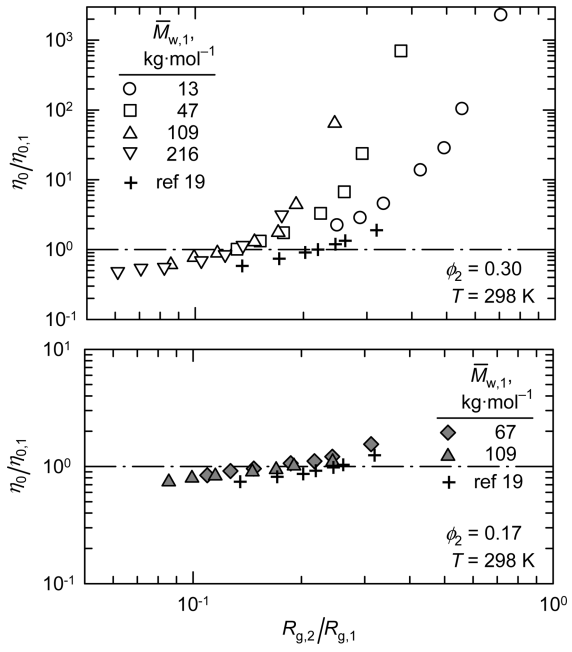

Figure 7. Relative viscosity of PDMS nanocomposites at 298 K as a function of the ratio of polysilicate R_g to PDMS R_g and nanoparticle volume fraction. Data from ref 19 obtained from a polydisperse polysilicate.

plasticization effect by the nanoparticles on viscosity would imply that d_t would increase by $\phi_1^{-\nu/(3\nu-1)}$ where ν is the Flory scaling exponent relating R_g to the degree of polymerization. SANS analysis of single chain dimensions from isotopic PDMS blends containing a soft polysilicate ($R_{g,2}$ = 1.1 nm) found $R_{g,1}$ decreased for chains approximately three times the nanoparticle size in the regime $M < M_c$. However, for chains with $M > M_c$, $R_{g,1}$ increased relative to its unperturbed dimensions.[66,67] SANS was also applied finding chain expansion in PNCs based on PS ($M > M_c$) such that $R/R_{g,1}$ ($\phi_1 = 1$) < 1 and $R_{g,1}$ ($\phi_1 \geq 0.90$)/$R_{g,1}$ ($\phi_1 = 1$) $\sim \phi_1^{-\alpha}$ where α appeared to be greater than unity.[31,68]

Modeling efforts yielded inconsistent trends primarily from restrictions placed on chain lengths and entanglements, and the immobilization of the filler particles. Ozmusul et al.[59] used lattice MC simulations to evaluate the role of h on chain conformation and on the statistics of bridges, loops, tails, and trains to assert that $R_{g,1}$ remained unaffected in the range $\phi_2 \leq 0.27$ and $1 \leq R_{g,1}/h \leq 4$. Rotational isomeric state MC studies found a $R/R_{g,1}$ dependence on the contraction or expansion of phantom chains.[69−71] MC[55−58,72] and MD[61] simulations predicted decreases in $R_{g,1}$ even for the condition $R < R_{g,1}$. From those studies, it is conceivable that the simulated rearrangement of chain segments to form bridges between nanoparticles is mechanistically responsible for the experimental results here using the 13K polymer where $R < R_{g,1}$ for the entire range of polysilicate nanoparticles and only reinforcement in terms of $\eta_0/\eta_{0,1} > 1$ was observed.

MC results by Termonia[60,73] revealed that chain expansion in the presence of nanoparticles is plausible. The condition $R_{g,1}/(R + h) > 2$ was found to be necessary for swelling; otherwise, contraction would be predicted in agreement with the experimental analysis by Nakatani et al.[66,67] Using simulated PNCs built from the same chemical structural building unit, Erguney et al.[74] also demonstrated conditions necessary for expansion and contraction of matrix chains, and reported that when the nanoparticle size was comparable or smaller, significant expansion on the order of $R_{g,1}$ (ϕ_1)/$R_{g,1}$ ($\phi_1 = 1$) $\sim \phi_1^{-1.2}$ was found.[75] It should be noted that both these simulations were consistent with the PS-based PNC experimental systems when the PS nanoparticles were $R \leq 2.7$ nm.[68]

All these effects on the unperturbed dimensions lead to a proposed generalized expression for the crossover size ratio from plasticization to reinforcement in the form of $\phi_1^{\alpha}(R_{g,2} + \delta)/R_{g,1}$, wherein α and δ should warrant more theoretical and experimental scrutiny.

Effect of Particle Size Distribution and Temperature. In the companion paper,[19] a polydisperse form of polysilicate designated R2 ($\overline{M}_w$ = 5.6 kg·mol^{-1}; $\overline{M}_w/\overline{M}_n$ = 2) was blended with narrow M fractions of PDMS to elucidate its effect on the $\eta_0 \sim \overline{M}_{w,1}$ relationship. This polysilicate was characterized by SANS to have $R_{g,2} = 1.5 \pm 0.3$ nm with a predominantly spherical shape.[18] Figure 7 compares the $\eta_0/\eta_{0,1} - R_{g,2}/R_{g,1}$ data for R2 (+) as a function of ϕ_2 at 298 K. The critical size ratio for viscosity reduction shifted to higher $R_{g,2}/R_{g,1}$: approximately 0.25 and 0.22 for ϕ_2 = 0.17 and ϕ_2 = 0.30, respectively. The shift is proposed to be primarily due to a broader polydispersity that increases ϕ_m, the ultimate effect from which is a reduction in $\eta_0/\eta_{0,1}$ whether considering viscosity models based on unimodal[76,77] or multimodal suspensions.[8−10]

The influence of polydispersity on $\eta_0/\eta_{0,1}$ also increased with ϕ_2. Using PNCs based on the 109K polymer for example, data obtained with the R2 polysilicate were $\eta_0(\phi_2 = 0.17)/\eta_{0,1}$ = 0.813 and $\eta_0(\phi_2 = 0.30)/\eta_{0,1}$ = 0.735. From Tables 2 and 4, a more appreciable decrease in $\eta_0/\eta_{0,1}$ was achieved at the higher $\phi_2$with the polydisperse R2 nanoparticle compared to the S4 (similar $\overline{M}_w$) and S7 (similar R_g) fractions. The impact from polydispersity increasing ϕ_m can be expected to be moderated by the increasing asymmetry of the nanoparticle.

Finally, it should be mentioned that the R2-based PNC η_0 was also measured at 353 K.[19] The effects from increasing temperature on the proposed mechanisms for viscosity reduction include (1) an increase in free volume; (2) a decrease in the lifetime of entanglements; and, (3) a weakening in the nanoparticle−polymer interactions. With data only available for PDMS,[45] $R_{g,1}$ was adjusted for temperature. This correction resulted in less than a 2% change in $R_{g,2}/R_{g,1}$ and did not appear to significantly alter the results within experimental error. There would be presumably less of a thermal effect on the rigid nanoparticle, and any adjustment of $R_{g,2}$ would lessen the change in $R_{g,2}/R_{g,1}$.

Increasing the temperature from 298 to 353 K shifted the crossover ratio higher $R_{g,2}/R_{g,1}$ of 0.30 and 0.26 for ϕ_2 = 0.17 and ϕ_2 = 0.30, respectively. The shift was comparable at both nanoparticle concentrations thereby suggesting a primary contribution from the temperature dependence of viscosity and free volume. This can be shown by using the data from ϕ_2 = 0.17 as an example and 298 K as the reference temperature ($R_{g,2}/R_{g,1}$ = 0.25). The crossover at 353 K would occur at $R_{g,2}/R_{g,1}$ = 0.24 if the relative viscosity was normalized by temperature $\eta_0 T/\eta_{0,1}$ assuming a constant, Arrhenius-type activation energy for viscous flow over this temperature range.

Conclusions

This experimental study focused on the effect of molecular size on the zero-shear-rate viscosity of PDMS-polysilicate nanocomposites. This PNC system was attractive as a model for study since the components are compatible over broad compositional ranges, the PDMS backbone flexibility allows PNCs that flow at room temperature over broad molecular weight ranges and strong, specific particle−polymer interactions are avoided which may otherwise dominate the behavior.

Seven narrow molecular-weight fractions of a trimethylsilyl-treated polysilicate were obtained by supercritical fluid extraction. Small-angle neutron scattering experiments revealed that the polysilicates evolved from spherically- to cylindrically shaped rigid nanoparticles as the radius of gyration increased from 0.75 to 2.1 nm. The viscous response of the PNCs, prepared using five entangled polymers filled by each of the polysilicate nanoparticle fractions at two concentrations, were characterized. A monotonic increase in viscosity with increasing nanoparticle size was observed for a polymer below its critical molecular weight for chain entanglement effects to impact viscosity. Above this critical molecular weight, the PNC viscosity was either lower or higher than the base polymer. The transition from plasticization (viscosity reduction) to reinforcement (viscosity increase) occurred at a particle-to-polymer size ratio less than unity. The critical nanoparticle-to-polymer R_g ratio at 298 K was 0.18 ± 0.006 and 0.13 ± 0.003 for a nanoparticle volume fraction of 0.17 and 0.30, respectively. The effects of nanoparticle concentration and polydispersity as well as temperature were discussed and compared to numerous published results on PNCs.

Acknowledgment. R.G.S. and G.V.G. acknowledge A. L. Tanke and L. L. Myers for material characterization. C.A.D. and T.C. acknowledge the HMI, Berlin, for the provision of beam time and the European Commission for financial support under the sixth Framework Programme through the Key Action: Strengthening the European Research Infrastructures (Contract No. RII3-CT-2003-505925 (NMI 3)).

References and Notes

(1) Einstein, A. *Ann. Phys.* **1906**, *19*, 289–306.
(2) Einstein, A. *Ann. Phys.* **1911**, *34*, 591–592.
(3) Smallwood, H. M. *J. Appl. Phys.* **1944**, *15*, 758–766.
(4) Nielsen, L. E.; Landel, R. F. *Mechanical Properties of Polymers and Composites*, 2nd ed.; Marcel Dekker: New York, 1994.
(5) Cumberland, D. J.; Crawford, R. J. *The Packing of Particles; Handbook of Powder Technology Vol. 6*; Elsevier: Amsterdam, 1987.
(6) Thomas, D. G. *J. Colloid Sci.* **1965**, *20*, 267–277.
(7) Lewis, T. B.; Nielsen, L. E. *Trans. Soc. Rheol.* **1968**, *12*, 421–443.
(8) Chong, J. S. Ph.D. Thesis. University of Utah, 1962.
(9) Farris, R. J. *Trans. Soc. Rheol.* **1968**, *12*, 281–301.
(10) Chong, J. S.; Christiansen, E. B.; Baer, A. D. *J. Appl. Polym. Sci.* **1971**, *15*, 2007–2021.
(11) Prokopenko, V. V.; Petkevich, O. K.; Malinskii, Yu. M.; Bakeev, N. F. *Dokl. Akad. Nauk SSSR* **1974**, *214*, 389–392.
(12) Guzeev, V. V.; Rafikov, M. N.; Malinskii, Yu. M. *Vysokomol. Soed., Ser. A* **1975**, *17*, 804–806.
(13) Prokopenko, V. V.; Titova, O. K.; Fesik, N. S.; Malinskii, Yu. M.; Bakeev, N. F. *Vysokomol. Soed., Ser. A* **1977**, *19*, 95–101.
(14) Guzeev, V. V.; Rafikov, M. N.; Malinskii, Yu. M. *Vysokomol. Soed., Ser. B* **1978**, *20*, 387–388.
(15) Roberts, C. H. Ph.D. Thesis. University of Bristol, Bristol, U.K., Sep. 2000.
(16) Cosgrove, T.; Roberts, C.; Choi, Y.; Schmidt, R. G.; Gordon, G. V.; Goodwin, A. J.; Kretschmer, A. *Langmuir* **2002**, *18*, 10075–10079.
(17) Roberts, C.; Cosgrove, T.; Schmidt, R. G.; Gordon, G. V.; Goodwin., A. J.; Kretschmer, A. In *Synthesis and Properties of Silicones and Silicone-Modified Materials*; Clarson, S. J., Fitzgerald, J. J., Owen, M. J., Smith, S. D., Van Dyke, M. E., Eds.; ACS Symposium Series 838; American Chemical Society: Washington, DC, 2003; pp 181−192.
(18) Benton, N. J. Ph.D. Thesis. University of Bristol, Bristol, U.K., Sep. 2004.
(19) Schmidt, R. G.; Gordon, G. V.; Quintero, M.; Benton, N. J.; Cosgrove, T.; Krukonis, V. J.; Williams, K.; Wetmore, P. M. *Macromolecules*.DOI: 10.1021/ma100490c.
(20) Mackay, M. E.; Dao, T. T.; Tuteja, A.; Ho, D. L.; Van Horn, B.; Kim, H.-C.; Hawker, C. *J. Nat. Mater.* **2003**, *2*, 762–766.
(21) Tuteja, A.; Mackay, M. E.; Hawker, C. J.; Van Horn, B. *Macromolecules* **2005**, *38*, 8000–8011.
(22) Tuteja, A.; Duxbury, P. M.; Mackay, M. E. *Macromolecules* **2007**, *40*, 9427–9434.
(23) Tuteja, A.; Mackay, M. E.; Narayanan, S.; Asokan, S.; Wong, M. S. *Nano Lett.* **2007**, *7*, 1276–1281.
(24) Kopesky, E. T.; Haddad, T. S.; Cohen, R. E.; McKinley, G. H. *Macromolecules* **2004**, *37*, 8992–9004.
(25) Jordan, J.; Jacob, K. I.; Tannenbaum, R.; Sharaf, M. A.; Jasiuk, I. *Mat. Sci. Eng.* **2005**, *393*, 1–11.
(26) Ganesan, V.; Pryamitsyn, V.; Surve, M.; Narayanan, B. *J. Chem. Phys.* **2006**, *124* (22); Art. No. 221102.
(27) Kairn, T.; Davis, P. J.; Ivanov, I.; Bhattacharya, S. N. *J. Chem. Phys.* **2005**, *123* (19); Art. No. 194905.
(28) de Gennes, P. G. *J. Chem. Phys.* **1971**, *55*, 572–579.
(29) Doi, M.; Edwards, S. F. *The Theory of Polymer Dynamics*: Clarendon Press: Oxford, 1986.
(30) Schmidt, R. G.; Badour, L. R.; Gordon, G. V. *Polym. Preprints* 2001, *42*(1), 112−113; In *Synthesis and Properties of Silicones and Silicone-Modified Materials*; Clarson, S. J., Fitzgerald, J. J., Owen, M. J., Smith, S. D., Van Dyke, M. E., Eds.; ACS Symposium Series 838; American Chemical Society: Washington, DC, 2003; pp 170−180.
(31) Mackay, M. E.; Tuteja, A.; Duxbury, P. M.; Hawker, C. J.; Van Horn, B.; Guan, Z.; Chen, G.; Krishnan, R. S. *Science* **2006**, *311*, 1740–1743.
(32) Cosgrove, T. *Macromolecules* **1982**, *15*, 1290–1293.
(33) Graessley, W. W. *Adv. Polym. Sci.* **1982**, *47*, 67–117.
(34) Liu, J.; Cao, D.; Zhang, L. *J. Phys. Chem. C* **2008**, *112*, 6653–6661.
(35) Smith, G. D.; Bedrov, D.; Li, L.; Byutner, O. *J. Chem. Phys.* **2002**, *117*, 9478–9489.
(36) Pryamitsyn, V.; Ganesan, V. *J. Rheol.* **2006**, *50*, 655–683.
(37) Brochard Wyart, F.; de Gennes, P. G. *Eur. Phys. J. E* **2000**, *1*, 93–97.
(38) Sen, S.; Thomin, J. D.; Kumar, S. K.; Keblinksi, P. *Macromolecules* **2007**, *40*, 4059–4067.
(39) Desai, T.; Keblinksi, P.; Kumar, S. K. *J. Chem. Phys.* **2005**, *122*; Art. No. 134910.
(40) Li, G.; Wang, L.; Ni, H.; Pittman, C. U., Jr. *J. Inorg. Organomet. Polym.* **2002**, *11*, 123–154.
(41) Merrill, D. F. *Adhes. Age* **1979**, *22* (3), 39–41.
(42) *Handbook of Pressure-Sensitive Adhesive Technology*; Satas, D., Ed.; Van Nostrand Reinhold: New York, 1982: Chapters 15 and 18.
(43) Daudt, W.; Tyler, L. U.S. Patent 2,676,182, 1954.
(44) McHugh, M. A.; Krukonis, V. J. *Supercritical Fluid Extraction: Principles and Practices*, 2nd ed.; Butterworth-Heinemann: Boston, MA, 1994; Chapter 9.
(45) Fetters, L. J.; Lohse, D. J.; Richter, D.; Witten, T. A.; Zirkel, A. *Macromolecules* **1994**, *27*, 4639–4647.
(46) Langley, N. R.; Mbah, G. C.; Freeman, H. A.; Huang, H.-H.; Siochi, E. J.; Ward, T. C.; Wilkes, G. *J. Colloid Interface Sci.* **1991**, *143*, 309–317.
(47) Guinier, A. *Ann. Phys.* (*Paris*) **1939**, *12*, 161–237.
(48) *Neutron, X-rays and Light. Scattering Methods Applied to Soft Condensed Matter*; Lindner, P.; Zemb, Th., Ed.; Elsevier: Amsterdam, 2002.
(49) Friedman, E. M.; Porter, R. S. *Trans. Soc. Rheol.* **1975**, *19*, 493–508.
(50) Roberts, C.; Cosgrove, T.; Schmidt, R. G.; Gordon, G. V. *Macromolecules* **2001**, *34*, 538–543.
(51) Rubinstein, M.; Colby, R. H. *Polymer Physics*; Oxford: Oxford, U. K., 2003; Chapter 9.
(52) Cosgrove, T.; Griffiths, P. C.; Lloyd, P. M. *Langmuir* **1995**, *11*, 1457–1463.
(53) Cosgrove, T.; Turner, M. J.; Weatherhead, I.; Roberts, C.; Garasanin, T.; Schmidt, R. G.; Gordon, G. V.; Hannington, J. P..In *Silicones and Silicone-Modified Materials*; Clarson, S. J.; Fitzgerald, J. J.; Owen, M. J.; Smith, S. D., Eds.; ACS Symposium Series 729, American Chemical Society: Washington, DC, 2000; pp 204−213.
(54) Surve, M.; Pryamitsyn, V.; Ganesan, V. *Langmuir* **2006**, *22*, 969–981.
(55) Vacatello, M. *Macromolecules* **2001**, *34*, 1946–1952.
(56) Vacatello, M. *Macromolecules* **2002**, *35*, 8191–8193.
(57) Vacatello, M. *Macromol. Theory Simul.* **2003**, *12*, 86–91.
(58) Ozmusul, M. S.; Picu, C. R. *Polymer* **2002**, *43*, 4657–4665.
(59) Ozmusul, M. S.; Picu, C. R.; Sternstein, S. S.; Kumar, S. K. *Macromolecules* **2005**, *38*, 4495–4500.
(60) Termonia, Y. *Polymer* **2009**, *50*, 1062–1066.
(61) Starr, F. W.; Schrøder, T. B.; Glotzer, S. C. *Macromolecules* **2002**, *35*, 4481–4492.
(62) Brown, D.; Marcadon, V.; Mélé, P.; Albérola, N. D. *Macromolecules* **2008**, *41*, 1499–1511.
(63) de Gennes, P. G. *Scaling Concepts in Polymer Physics*: Cornell University: Ithaca, NY, 1979 ; Chapter 6.

(64) Garvey, M. J.; Tadros, T. F.; Vincent, B. J. *J. Colloid Interface Sci.* **1974**, *49*, 57–68.
(65) Cosgrove, T.; Luckham, P. F.; Richardson, R. M.; Webster, J. R. P.; Zarbakhsh, A. *Colloids Surf. A* **1994**, *86*, 103–110.
(66) Nakatani, A. I.; Chen, W.; Schmidt, R. G.; Gordon, G. V.; Han, C. C. *Polymer* **2001**, *42*, 3713–3722.
(67) Nakatani, A. I.; Chen, W.; Schmidt, R. G.; Gordon, G. V.; Han, C. C. *Int. J. Thermophys.* **2002**, *23*, 199–209.
(68) Tuteja, A.; Duxbury, P. M.; Mackay, M. E. *Phys. Rev. Lett.* **2008**, *100*, 077801(4).
(69) Kloczkowski, A.; Sharaf, M. A.; Mark, J. E. *Chem. Eng. Sci.* **1994**, *49*, 2889–2897.
(70) Yuan, Q. W.; Kloczkowski, A.; Mark, J. E.; Sharaf, M. A. *J. Polym. Sci., Polym. Phys.* **1996**, *34*, 1647–1657.
(71) Sharaf, M. A.; Mark, J. E. *Polymer* **2004**, *45*, 3943–3952.
(72) Picu, C. R.; Ozmusul, M. S. *J. Chem. Phys.* **2003**, *118*, 11239–11248.
(73) Termonia, Y. *J. Polym. Sci., Polym. Phys.* **2010**, *48*, 687–692.
(74) Erguney, F. M.; Lin, H.; Mattice, W. L. *Polymer* **2006**, *47*, 3689–3695.
(75) Erguney, F. M.; Mattice, W. L. *Polymer* **2008**, *49*, 2621–2623.
(76) Mooney, M. *J. Colloid Sci.* **1951**, *6*, 162–170.
(77) Krieger, I. M.; Dougherty, T. J. *Trans. Soc. Rheol.* **1959**, *3*, 137–152.